Electronic Supplementary Material (ESI) for Nanoscale.
This journal is © The Royal Society of Chemistry 2016

Electronic Supplementary Material

Distinguishing Uniform Switching from Filamentary Switching in Resistance Memory Using a Fracture Test

Yang Lu, Jong Ho Lee, Xiang Yang and I-Wei Chen

Department of Materials Science and Engineering, University of Pennsylvania

Philadelphia, PA 19104-6272, USA

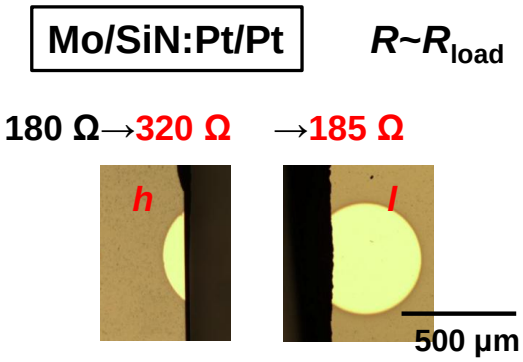

Figure S1. One severed Mo/Si_3N_4:Pt/Pt pairs from initially intact LRS device with R_0=180 Ω (R_0A_0=37.1 Ωmm^2) very close to load resistance R_{load}=150 Ω. R= 320 Ω in one piece (A/A_0~14%, RA=9.2 Ωmm^2), and R=185 Ω in the other pice (A/A_0~82%, RA=31.2 Ωmm^2). Resistance read at 0.1 V.

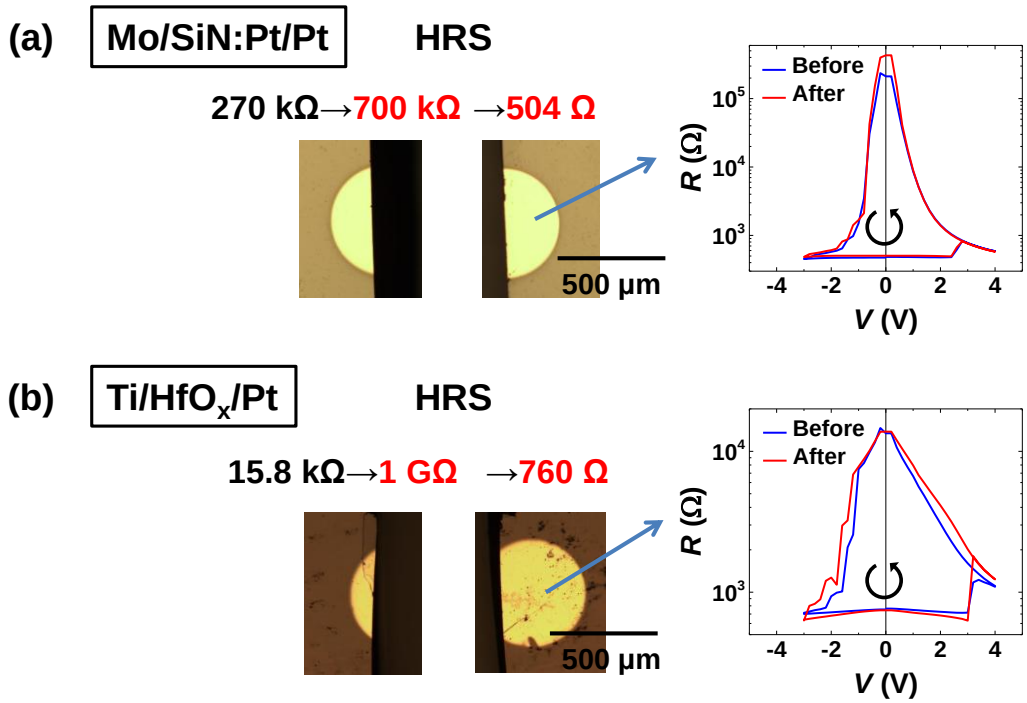

Figure S2. Severed (a) Mo/Si_3N_4:Pt/Pt pair and (b) Ti/HfO_x/Pt pair from initially intact HRS devices. Stress-induced HRS→LRS switching during fracture observed in less resistive pieces in both sets. As indicated by arrows, the switching curves of these stress-induced LRS states (red curves, after) are similar to the switching curves of the initial, intact devices (blue, before). The HRS in these curves is area-dependent in Mo/Si_3N_4:Pt/Pt, but not in Ti/HfO_x/Pt.

Mechanical switching and electron-phonon interactions (ref. S4)

Pressure-induced switching in the absence of any electrical stimulus is a direct evidence of electron-phonon interaction, which is thought to stabilize the trapped charge that gives rise to the HRS in nanometallic RRAM in the following way. (a) Localized electron-phonon interaction at certain sites (negative-*U* sites) lowers the energy of a newly added second electron therein, thus trapping it. (b) When the interaction, manifested by local bond distortion, is reversed by a pressure, the trapped electron is destabilized, thus leaves the trapping site. (c) Since the trapped

electron can erect a Coulomb barrier to blocked itinerant electrons, it gives rise to HRS; conversely, detrapping triggers the transition from HRS to LRS, which has fewer or no trapped electrons. (IRS has some intermediate number of trapped electrons.) (d) Only the second (paired) electron can feel the negative-U energy, so the pressure effect is not felt when there is no such electron, *i.e.*, pressure cannot induce the LRS→HRS transition.

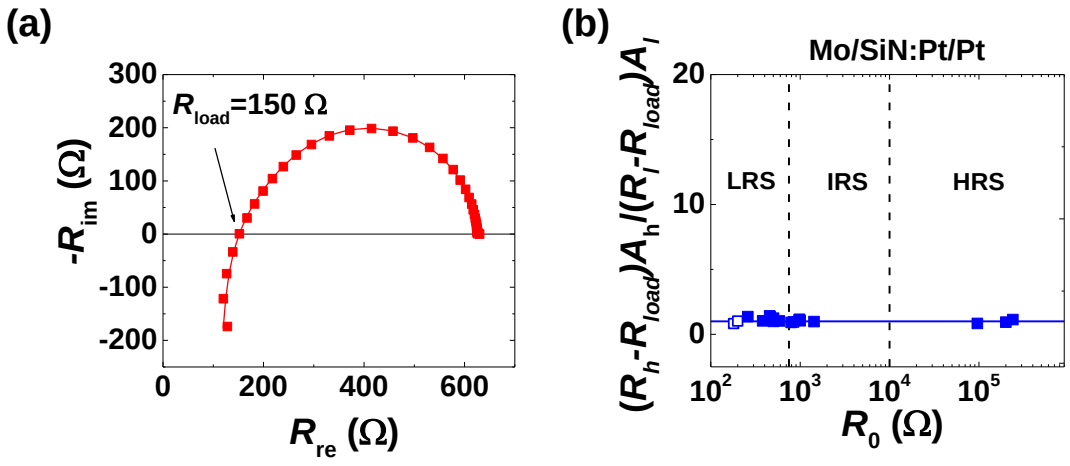

Figure S3. Error analysis of *R* for Mo/Si_3N_4:Pt/Pt. (a) Electrode spreading resistance R_{load} determined by impedance spectroscopy showing Cole-Cole plot of LRS of Mo/Si_3N_4:Pt/Pt with an intercept at R_{load}=150 Ω. (b) Data points of Mo/Si_3N_4:Pt/Pt in **Fig. 4(a)** replotted as $(R_h\text{-}R_{load})A_h/(R_l\text{-}R_{load})A_l$ to exclude R_{load}. Most data (filled symbols) satisfy $R_0>>R_{load}$ but data with $R_0\sim R_{load}$ (hollow symbols) behave similarly.

Our Mo/Si_3N_4:Pt/Pt devices have an area-insensitive spreading resistance R_E in the bottom electrode, which is thin.[1-3] This resistance is determined in **Fig. S3a**, and is about $R_E\sim R_{load}$ =150 Ω, using impedance spectroscopy. (See refs. S4-5 for detailed fitting parameters and equivalent circuit.) This resistance R_{load} is a part of both R_h and R_l. Its effect is small especially if R_h and R_l are large. In some figures such as **Fig. 4(a)**, consideration of this correction barely changes the correlation as can be seen by comparing **Fig. S3(b)**, which plots $(R_h\text{-}R_{load})A_h/(R_l\text{-}R_{load})A_l$, with **Fig. 4(a)**, which plots R/R_0. The error ε due to R_{load} is

$$\varepsilon = \frac{\frac{(R_h - R_{load})A_h}{(R_l - R_{load})A_l} - \frac{R_h A_h}{R_l A_l}}{\frac{R_h A_h}{R_l A_l}} = \frac{(R_h - R_{load})A_h}{(R_l - R_{load})A_l} \times \frac{R_l A_l}{R_h A_h} - 1 = \frac{1 - \frac{R_{load}}{R_h}}{1 - \frac{R_{load}}{R_l}} - 1$$

It is easy to see that $|\varepsilon|$ decreases as R increases. Specifically, if $R>>R_{load}$,

$$|\varepsilon|_{\max} \approx \frac{R_{load}}{R_l} - \frac{R_{load}}{R_h}$$

References

S1. A. B. Chen, B. J. Choi, X. Yang, I. W. Chen, *Adv. Funct. Mater.* **22,** 546-554 (2012).

S2. X. Yang, I. W. Chen, I. W, *Sci. Rep.* **2,** 744 (2012).

S3. X. Yang, A. B. Chen, B. J. Choi, I. W. Chen, *Appl. Phys. Lett*. **102,** 043502 (2013).

S4. X. Yang, I. Tudosa, B. J. Choi, A. B. Chen, and I. W. Chen, *Nano Lett.* **14,** 5058 (2014).

S5. Y. Lu, J. H. Lee, and I. W. Chen, *ACS nano* **9,** 7649-7660 (2015).